

CLASS SIMILARITY-BASED MULTIMODAL CLASSIFICATION UNDER HETEROGENEOUS CATEGORY SETS

Yangrui Zhu*

School of Computer Science
Wuhan University
Wuhan, China
yangruizhu@whu.edu.cn

Junhua Bao*

School of Computer Science
Wuhan University
Wuhan, China
junhuabao@whu.edu.cn

Yipan Wei

School of Computer Science
Wuhan University
Wuhan, China
yipawei@whu.edu.cn

Yapeng Li†

School of Computer Science
Wuhan University
Wuhan, China
yapengli@whu.edu.cn

Bo Du†

School of Computer Science
Wuhan University
Wuhan, China
boddu@whu.edu.cn

ABSTRACT

Existing multimodal methods typically assume that different modalities share the same category set. However, in real-world applications, the category distributions in multimodal data exhibit inconsistencies, which can hinder the model’s ability to effectively utilize cross-modal information for recognizing all categories. In this work, we propose the practical setting termed Multi-Modal Heterogeneous Category-set Learning (MMHCL), where models are trained in heterogeneous category sets of multi-modal data and aim to recognize complete classes set of all modalities during test. To effectively address this task, we propose a Class Similarity-based Cross-modal Fusion model (CSCF). Specifically, CSCF aligns modality-specific features to a shared semantic space to enable knowledge transfer between seen and unseen classes. It then selects the most discriminative modality for decision fusion through uncertainty estimation. Finally, it integrates cross-modal information based on class similarity, where the auxiliary modality refines the prediction of the dominant one. Experimental results show that our method significantly outperforms existing state-of-the-art (SOTA) approaches on multiple benchmark datasets, effectively addressing the MMHCL task.

1 Introduction

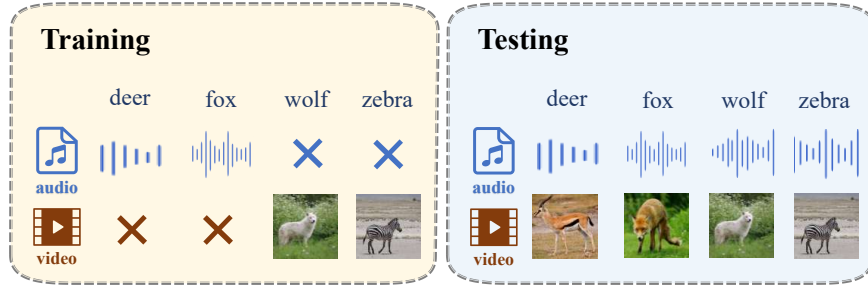
In real-world applications, due to limitations in equipment, time costs, and budget, datasets are typically collected for specific tasks. For example, a project focused on video animal classification may only collect video data, while a project developing an audio action recognition system may primarily collect audio data. However, from a multimodal learning perspective, both video and audio data can inherently provide valuable information for these recognition tasks. This leads to a critical research question: **Can a unified multimodal recognition model be constructed by integrating modality data from heterogeneous category sets?** Such a model needs not only to handle all relevant modality data but also to recognize the complete category set.

To address this, we propose a new paradigm called Multi-Modal Heterogeneous Category-set Learning (MMHCL, as shown in Figure 1a).

Current related research has three main limitations: First, traditional multimodal classification methods [2, 4] can enhance performance through modality complementarity, but their basic assumption requires that all modality data must cover all categories (as shown in Figure 2b), making them incapable of handling data missing at the category level. Second, incomplete multi-view classification methods [5, 3, 6, 7] address modality missing at the sample level (as shown in Figure 2c), but they also lack solutions for missing data at the category level. Third, zero-shot learning methods enable recognition of unseen categories through generation mechanisms or feature alignment, but they fail to

*Equal contribution.

†Corresponding author.



(a) Our Setting

Dataset	DGZ [1]	TMC [2]	UVaT [3]	Ours
ActivityNet	31.11	32.72	35.48	45.71

(b) Results

Figure 1: Setting illustration and results: (a) Setup for MMHCL. During the training phase, each modality has an inconsistent category set, with X indicating categories not covered by each modality. In the testing phase, the model needs to recognize the complete category space across all modalities. (b) Performance comparison on the ActivityNet dataset (Real-world Scenarios) under MMHCL scenario. Our method significantly outperforms existing SOTA approaches.

effectively leverage the complementary advantages of multimodal data [1, 8, 9] or requires that all modality data must be complete [10, 11, 12, 13].

Therefore, we aim to develop a method that can effectively enhance robustness in addressing the MMHCL task.

To achieve this goal, we are confronted with three main challenges: 1) How to enable unimodal data, which only includes part of the categories, to recognize the complete category set including unseen classes; 2) In a multimodal prediction scenario, how to accurately identify the modality domain of the data and allow the corresponding modality to dominate the fusion decision; 3) How to effectively utilize complementary information from other modalities to assist the dominant modality’s prediction. To address these challenges, we propose a Class Similarity-based Cross-modal Fusion model (CSCF), which is trained on modality-specific data with heterogeneous category sets and is capable of recognizing the complete category space across all modalities. Specifically, we enhance category semantic representation through large language models (LLM), constructing a unified semantic space as a bridge between seen and unseen categories. We map data from each modality to this semantic space and leverage the semantic correlations between categories to facilitate knowledge transfer, enabling generalization to unseen categories (**challenge 1**).

Furthermore, we design uncertainty estimation to assess prediction inconsistencies among sub-modules and differences across modalities in a dynamic and robust manner, thus determining the dominant modality and ensuring that the fusion decision is driven by the most discriminative modality (**challenge 2**). Finally, guided by class semantic similarity, we adaptively fuse complementary information from other modalities to enhance overall prediction capability (**challenge 3**).

To summarize, the contributions of this paper are as follows:

- To the best of our knowledge, this is the first study on MMHCL, which utilizes multimodal data with different category sets to develop a model capable of recognizing all categories across all modalities.
- We propose a Class Similarity-based Cross-modal Fusion model (CSCF), which requires only one training session and can simultaneously integrate cross-modal information and recognize complete category space across all modalities.
- We find that leveraging semantic discriminability, modality prediction consistency, and class semantic similarity is crucial to solving this problem.

We conduct extensive experiments on diverse real-world datasets. The results show that in the practical MMHCL setting, our method significantly outperforms the most competitive counterpart by 10.23%, 10.77%, and 3.30% on the ActivityNet, UCF, and VGGSound datasets, respectively.

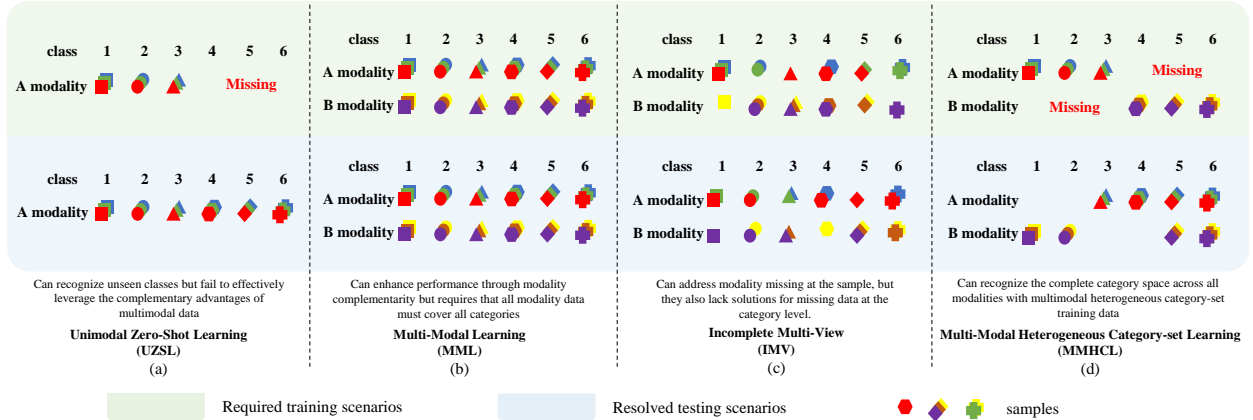


Figure 2: Comparison of Settings. Unimodal Zero-shot learning (UZSL) focuses on seen classes and unseen classes within a single modality, making it unsuitable for cross-modal scenarios. Multimodal learning (MML) requires all modality data to cover all categories during training, and testing is conducted on complete samples with seen classes. Incomplete view (IMV) classification allows for modalities missing at the sample level both training and testing but lack solutions for missing data at the category level. Under our proposed setting (MMHCL), the training data exhibits inconsistent class coverage across modalities, and the model is required to recognize the complete category space across all modalities.

2 Related Work

2.1 Multimodal Learning

To fully utilize the information from different modalities, multimodal learning [14, 15, 16, 17, 18, 19, 20, 21] has become a widely researched field. Based on different fusion strategies, multimodal learning methods can generally be divided into three categories: early fusion [22, 23], intermediate fusion [24, 25, 26, 27, 28, 29, 30, 31, 32, 33], and decision fusion [34, 35, 2, 36, 4, 37]. Early fusion based methods directly integrate multiple modalities at the data level, typically concatenating multimodal data. Intermediate fusion combines data from different modalities at intermediate layers of a neural network [24, 25, 26, 27, 28, 29, 30], effectively capturing the complementary information of each modality to enhance the model’s performance. Decision fusion typically involves the integration of multimodal data based on uncertainty evaluation [38, 39, 40], voting schemes [41], and so on [42, 43, 44, 45]. However, these multimodal methods assume that all modalities must cover all categories and use fully connected layers as classifiers. They only recognize the seen categories for each modality and cannot generalize to the unseen categories for each modality. In contrast, our approach uses semantics as a bridge to map data from each modality into a semantic space, enabling the recognition of unseen categories in each modality.

2.2 Incomplete Multi-View Classification

Incomplete multi-view classification has been widely studied to address the common problem of missing modality in some samples in real-world scenarios. Existing incomplete multi-view (IMV) learning methods can be roughly divided into two categories: model-independent methods [46, 47, 48] and model-based methods [49, 50, 5, 3, 51]. Model-independent methods generally involve a two-stage process to tackle the incomplete multi-view problem. In the first stage, a model-independent preprocessing strategy is designed (e.g., imputation [47, 48] or simply discarding samples with missing views) to construct a complete multi-view dataset. In the second stage, standard multi-view learning methods are applied to process the reconstructed complete data. On the other hand, model-based methods address the incomplete views problem by designing specific multi-view learning models based on traditional machine learning or deep learning. For example, LMVCAT [5] uses label-guided masked views and a category-aware transformer to avoid the negative impact of missing views on information interaction, while UVaT [3] employs a view-aware transformer to mask the missing views and adaptively explores the relationship between views and target tasks to handle missing views. However, these methods only consider modality missing at the sample level (some samples may lack certain modalities) but overlook the modality-category missing problem that arises in some scenarios (where certain modalities completely lack specific categories). This limitation causes a significant decline in model generalization when the test data contains categories unseen by a specific modality during training. In contrast, our method effectively solves the more challenging modality-category missing problem.

2.3 Generalized Zero-Shot Learning

Generalized Zero-Shot Learning (GZSL) can be broadly categorized into unimodal and multimodal approaches. In unimodal settings, the predominant methods fall into two paradigms: embedding-based [52, 53, 54, 55, 56, 57, 58, 8] and generation-based [59, 60, 61, 62, 63, 64, 65, 66, 1, 67]. Embedding-based methods aim to learn a shared embedding space that aligns visual and semantic features. By measuring similarity between the prototype of a seen class and the projected representation of a predicted class in this space, the model can recognize unseen categories. Generation-based methods, on the other hand, employ generative models to synthesize visual features or even images for unseen classes, conditioned on their semantic descriptions. This effectively transforms the GZSL problem into a standard supervised classification task. However, these unimodal methods fail to exploit the complementary information present in multimodal data. To address these challenges, researchers have proposed multimodal GZSL methods [10, 11, 12, 13]. For example: AVCA [11] employs a cross-attention mechanism to enable effective multimodal information fusion. CLIPCLAP [13] leverages high-quality features extracted from large-scale pretrained models such as CLIP and CLAP to enhance performance. Despite their advances, most existing methods rely on an idealized assumption: That multimodal data must be complete, which is often invalid in real-world applications where different modalities may cover distinct subsets of the category set. In contrast, our proposed method focuses on more realistic scenarios with modality incompleteness and category-set inconsistency, thereby improving the model’s practicality.

3 Method

Problem Formulation. In the MMHCL setup, we consider m modalities, denoted as $\mathcal{M} = \{M_1, M_2, \dots, M_m\}$. For each modality M_i , we define its seen category set as Y_s^i and unseen category set as Y_u^i . The corresponding data and labels are denoted as X^i and y^i , respectively. In practice, each modality covers only a subset of the total category space, and the seen category sets across modalities may partially overlap or be completely disjoint. Formally, we have: $\bigcup_{i=1}^m Y_s^i = \mathcal{Y}$, and $Y_s^i \cap Y_s^j \neq \emptyset$ or $Y_s^i \cap Y_s^j = \emptyset$, $\forall i \neq j$, where \mathcal{Y} denotes the union of all categories involved across modalities. Each training sample is represented as $\{X_k^i, y_k\}$, where $X_k^i \in X^i$ and $y_k \in \mathcal{Y}$, indicating that the k -th sample only exists in modality M_i , and data from other modalities is considered missing. Our objective is to train an end-to-end multimodal classifier that can recognize the complete category space across all modalities, given all modality-specific training data $\{X^1, \dots, X^m\}$ and their corresponding labels $\{y^1, \dots, y^m\}$. This work focuses on a fundamental yet challenging case with two modalities, where each modality corresponds to a disjoint set of categories.

Overall Framework. The proposed CSCF model is illustrated in Figure 3. From a unimodal perspective, the model is trained on seen classes and must generalize to unseen ones. To bridge this gap, we enhance class semantics using large language models (LLMs) [68] and map features into a shared semantic space (see the OSRS module in Figure 3). From a multimodal perspective, each modality covers only part of the category space, leading to varying prediction quality. So we design uncertainty estimation to identify the dominant modality for decision-making (see the DMSS module in Figure 3). Finally, we perform adaptive fusion guided by class semantic similarity, where auxiliary modality predictions refine the dominant modality’s output for comprehensive and accurate recognition (see the CSMF module in Figure 3).

3.1 Open Set Recognition via Semantics

Motivation of OSRS. In real-world scenarios, each modality only covers a subset of categories, requiring the model to recognize unseen classes from a unimodal perspective. We introduce class semantics as a bridge between seen and unseen classes. To enable knowledge transfer, we enhance semantic features using large language models (LLMs) and adopt the concept of open set recognition [69]. Modality-specific semantic mappers project features into a unified semantic space, allowing the model to leverage semantics for unseen class recognition.

Construction of OSRS. We use the semantic space as the shared alignment space. The feature \mathbf{x}^A from modality A is mapped to the semantic space via a mapper $A2S$, while the feature \mathbf{x}^B from modality B is mapped through $B2S$. The mapping process is defined as follows:

$$\begin{aligned} \mathbf{x}^A &\in \mathbb{R}^{N^A \times d^A} \xrightarrow{A2S} \hat{\mathbf{s}}^A \in \mathbb{R}^{N^A \times d^s}, \\ \mathbf{x}^B &\in \mathbb{R}^{N^B \times d^B} \xrightarrow{B2S} \hat{\mathbf{s}}^B \in \mathbb{R}^{N^B \times d^s}, \end{aligned} \quad (1)$$

where d^A and d^B are the input feature dimensions for the two modalities, and d^s is the output dimension aligned with the semantic feature space. $\hat{\mathbf{s}}^A$ and $\hat{\mathbf{s}}^B$ are the semantic features derived from the features of each modality. N^A and N^B denote the number of samples from seen classes in modalities A and B, respectively.

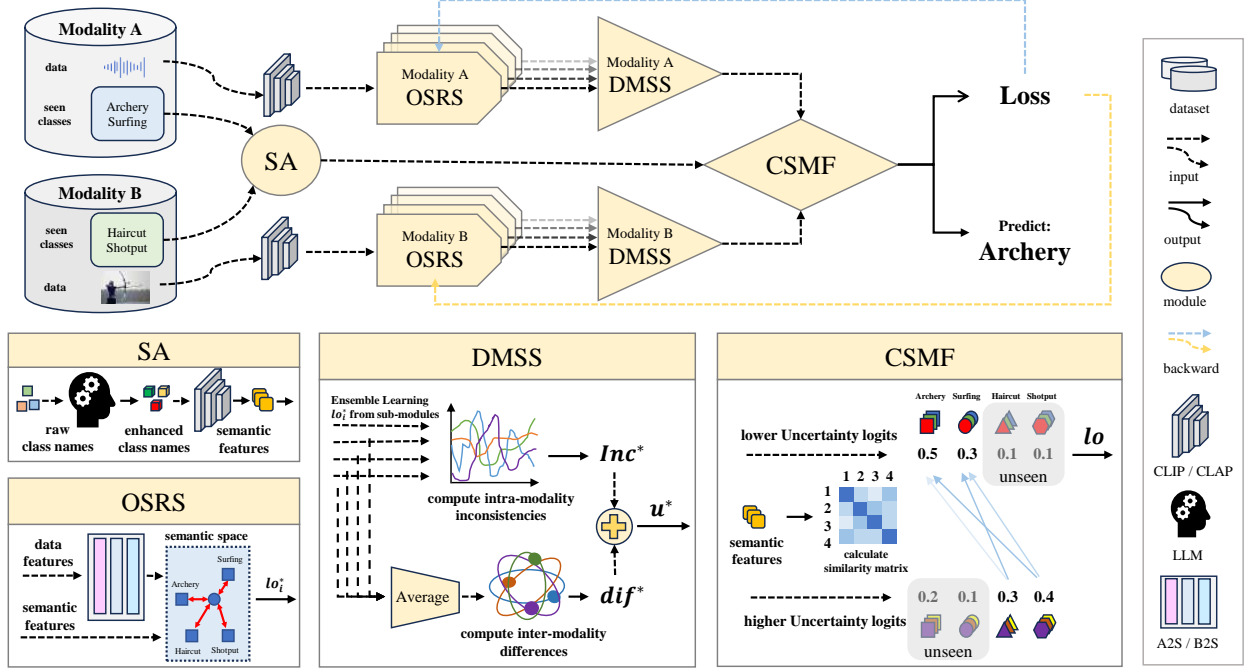


Figure 3: Overall framework of the proposed CSCF model. In the data processing phase, semantic enhancement is performed based on LLMs, and features are extracted using CLIP/CLAP. During training, our approach consists of three main modules: OSRS, DMSS, and CSMF. In the OSRS module, data features are mapped into the semantic space and classified based on distance. In the DMSS module, we consider both intra-modality inconsistencies and inter-modality differences of predictions, selecting the dominant modality to lead the prediction. In the CSMF module, we adaptively fuse multimodal predictions using class semantic similarity, where auxiliary modalities refine the dominant modality’s prediction. During inference, the model leverages all three modules to recognize the complete category space across all modalities.

Next, we compute the scaled cosine similarity between the modality-generated semantic features $\hat{\mathbf{s}}^*$ and the enhanced semantic features \mathbf{c}_i , where \mathbf{c}_i represents the enhanced semantic feature of the i -th class name (see appendix A for implementation details). The resulting similarity-based predictions \mathbf{lo}^* are computed as:

$$lo_i^* = \frac{\gamma^2 \hat{\mathbf{s}}^* \mathbf{c}_i}{\|\hat{\mathbf{s}}^*\| \|\mathbf{c}_i\|}, \quad (2)$$

$$\mathbf{lo}^* = [lo_1^*, lo_2^*, \dots, lo_N^*],$$

where $*$ denotes either modality A or B.

3.2 Dominant Modality Selection Strategy

Motivation of DMSS. In multimodal settings, each modality covers only part of the category space, making it difficult to achieve high-quality recognition individually, which affects the final fusion. Thus, the model must assess the reliability of each modality. Inspired by ensemble learning [70], we design uncertainty estimation to evaluate prediction quality. Empirically, OSRS modules within a modality show low inconsistency on seen classes and high inconsistency on unseen ones (see Appendix B). Based on this, we propose an entropy-based mechanism that measures intra-modality inconsistencies and inter-modality differences of predictions, enabling the model to dynamically select the dominant modality for robust fusion decisions.

Construction of DMSS. We apply ensemble learning by aggregating predictions from multiple OSRS modules and converting them into probability distributions:

$$\mathbf{lo}_i^* = OSRS_i(\mathbf{x}^*, \mathbf{c}), \quad (3)$$

$$\mathbf{p}_i^* = \text{softmax}(\mathbf{lo}_i^*),$$

where $*$ denotes modality A or B, i refers to the i -th OSRS module and \mathbf{c} represents for the semantic features of all classes. When predictions from multiple OSRS modules within a modality are lowly inconsistent, it indicates that the

modality can provide stable and reliable decisions for the current sample. To measure intra-modality disagreement of predictions, we use entropy-based inconsistency:

$$e^* = \sqrt{\frac{1}{K} \sum_{i=1}^K (H(\mathbf{p}_i^*) - \bar{H})^2}, \quad (4)$$

where $H(\mathbf{p}_i^*) = -\sum_{n=1}^N p_{i,n}^* \log p_{i,n}^*$ is the entropy of the i -th module’s prediction, and $\bar{H} = \frac{1}{K} \sum_{i=1}^K H(\mathbf{p}_i^*)$ is the mean entropy. The intra-modality inconsistency Inc^* for modality $*$ is then computed as:

$$Inc^* = \frac{e^*}{\sum_{* \in \{A, B\}} e^*}, \quad * \in \{A, B\}. \quad (5)$$

In addition, if the prediction from one modality significantly deviates from the others, it may indicate that the modality has captured critical discriminative information. To quantify this, we compute inter-modality prediction differences using entropy-based uncertainty estimation:

$$\begin{aligned} \mathbf{p}^* &= \text{softmax}\left(\frac{1}{K} \sum_{i=1}^K \mathbf{l}\mathbf{o}_i^*\right), \\ dif^* &= \frac{H(\mathbf{p}^*)}{\sum_{* \in \{A, B\}} H(\mathbf{p}^*)}, \quad * \in \{A, B\}. \end{aligned} \quad (6)$$

Finally, we combine intra-modality inconsistency and inter-modality prediction difference to compute the overall prediction uncertainty u^* for each modality:

$$u^* = Inc^* + dif^*, \quad (7)$$

where $*$ denotes modality A or B. The dominant modality usually corresponds to the one with the lower uncertainty (refer to Figure 7). By comparing u^A and u^B , the model can identify the dominant and auxiliary modalities, thereby enhancing the robustness of the final fusion decision.

3.3 Class Similarity-guided Multimodal Fusion

Motivation of CSMF. Different modalities vary in their ability to recognize certain classes. For example, the audio modality may better capture the neighing of a horse, while the video modality excels at identifying a donkey’s appearance. If the audio modality predicts “horse” and is selected as dominant by the DMSS module, the video prediction is still valuable due to the semantic similarity between “horse” and “donkey.” Thus, the auxiliary (video) modality’s prediction should be reasonably integrated to assist the dominant (audio) modality in making a more accurate decision. Motivated by this, we propose an adaptive fusion strategy guided by class semantic similarity. Predictions from the auxiliary modality are weighted based on their semantic relevance to the dominant modality’s prediction and then fused to improve overall classification. This mechanism not only leverages the strength of the dominant modality but also captures complementary information from auxiliary modalities.

Construction of CSMF. We concatenate the enhanced class semantic features \mathbf{c}_i to form the class semantic feature matrix \mathbf{C} , and compute cosine similarity between each pair of class semantics to obtain a similarity matrix $\mathbf{S} \in \mathbb{R}^{N \times N}$, where N is the number of classes:

$$\begin{aligned} \mathbf{C} &= [\mathbf{c}_1, \mathbf{c}_2, \dots, \mathbf{c}_N]^\top \in \mathbb{R}^{N \times d^s}, \\ S_{i,j} &= \cos(\mathbf{c}_i, \mathbf{c}_j) = \frac{\mathbf{c}_i^\top \mathbf{c}_j}{\|\mathbf{c}_i\|_2 \cdot \|\mathbf{c}_j\|_2}, \quad \forall i, j \in \{1, \dots, N\}. \end{aligned} \quad (8)$$

For modality $*$, we retain only the $top-k$ most semantically similar classes for each seen class, forming a pruned similarity matrix \mathbf{S}^* . The auxiliary modality’s predictions are then re-weighted according to this similarity matrix and added to the dominant modality’s predictions to yield the final prediction $\mathbf{l}\mathbf{o}$:

$$\begin{aligned} \tilde{\mathbf{l}}\mathbf{o}^A &= \mathbf{S}^A \cdot \mathbf{l}\mathbf{o}^A, \quad \tilde{\mathbf{l}}\mathbf{o}^B = \mathbf{S}^B \cdot \mathbf{l}\mathbf{o}^B, \\ \mathbf{l}\mathbf{o} &= \begin{cases} \mathbf{l}\mathbf{o}^A + \tilde{\mathbf{l}}\mathbf{o}^B, & \text{if } u^A < u^B, \\ \mathbf{l}\mathbf{o}^B + \tilde{\mathbf{l}}\mathbf{o}^A, & \text{otherwise,} \end{cases} \end{aligned} \quad (9)$$

where $\tilde{\mathbf{l}}\mathbf{o}^A$ and $\tilde{\mathbf{l}}\mathbf{o}^B$ are the similarity-enhanced components, and the fusion decision is dynamically made based on the prediction uncertainty u^* estimated by the DMSS module. Finally, the fused logits are converted into a probability distribution, enabling high-quality recognition across all categories.

Algorithm 1 Training Process of CSCF

Input: Training data X^A, Y_s^A and $\{X^B, Y_s^B\}$ from modalities A and B, semantic class features $\{\mathbf{c}_i\}_{i=1}^N$
Output: Trained parameters of A2S, B2S.
// Feature Extraction and Semantic Mapping
 $\mathbf{x}^A = \text{Backbone}_A(X^A), \quad \mathbf{x}^B = \text{Backbone}_B(X^B)$
 $\mathbf{c} = \text{CLIP}(\text{LLM}(Y))$
for $e = 1$ **to** E **do**
 $\hat{\mathbf{s}}^A = \text{A2S}(\mathbf{x}^A), \quad \hat{\mathbf{s}}^B = \text{B2S}(\mathbf{x}^B)$
// Ensemble OSRS: compute logits and probs
for $i = 1$ **to** K **do**
 $\mathbf{lo}_i^A, \mathbf{p}_i^A = \text{OSRS}_i(\hat{\mathbf{s}}^A, \mathbf{c}), \mathbf{lo}_i^B, \mathbf{p}_i^B = \text{OSRS}_i(\hat{\mathbf{s}}^B, \mathbf{c})$
end for
 $\mathbf{p}^A, \mathbf{p}^B \leftarrow \{(\mathbf{lo}_1^A, \dots, \mathbf{lo}_K^A), (\mathbf{lo}_1^B, \dots, \mathbf{lo}_K^B)\}$ in Eq.(3)
// DMSS: Compute modality uncertainty
 $\text{Inc}^A, \text{Inc}^B \leftarrow \{\mathbf{p}_1^A, \dots, \mathbf{p}_K^A; \mathbf{p}_1^B, \dots, \mathbf{p}_K^B\}$ in Eq.(4)
 $\text{dif}^A, \text{dif}^B \leftarrow \{\mathbf{p}^A, \mathbf{p}^B\}$ in Eq.(6)
 $u^A = \text{Inc}^A + \text{dif}^A, \quad u^B = \text{Inc}^B + \text{dif}^B$
// CSMF: Similarity-guided prediction fusion
 $\mathbf{S}_{i,j} = \frac{\mathbf{c}_i^\top \mathbf{c}_j}{\|\mathbf{c}_i\| \cdot \|\mathbf{c}_j\|}$
 $\mathbf{lo} \leftarrow \{\text{lo}^A, \text{lo}^B, \mathbf{S}^A, \mathbf{S}^B, u^A, u^B\}$ in Eq.(9)
// Compute total loss and update parameters
 $\mathcal{L} = \sum_{* \in \{A, B\}} (\frac{1}{K} \sum_{i=1}^K \text{CE}(\mathbf{p}_i^*, y) + \text{CE}(\mathbf{p}^*, y))$
Update parameters $\{\theta_{\text{A2S}_i, \text{B2S}_i}\}_{i=1}^K$ using Adam
end for

3.4 Training and Inference

During the training phase, the overall training objective \mathcal{L} is defined as:

$$\mathcal{L} = \sum_{* \in \{A, B\}} \left(\frac{1}{K} \sum_{i=1}^K \text{CE}(\mathbf{p}_i^*, y) + \text{CE}(\mathbf{p}^*, y) \right), \quad (10)$$

where $*$ denotes modality A or B, K is the number of OSRS modules, CE represents the cross-entropy loss function, \mathbf{p}_i^* is the prediction probability from the i -th OSRS module for modality $*$, \mathbf{p}^* is the average probability computed as in Equation (6), and y is the ground truth label. The complete training process is illustrated in Algorithm 1. At the end of each training epoch, the parameters of the A2S and B2S mappers are updated.

During inference, for each input multimodal sample, features are first extracted and then processed similarly to the training phase. The OSRS modules map each modality’s features into the semantic space via the corresponding mapper and computes similarity scores with all class semantics in Y to generate per-modality predictions. The DMSS module aggregates the predictions from multiple OSRS modules to evaluate intra-modality inconsistencies and inter-modality differences, thereby determining the dominant modality for fusion. Finally, the CSMF module performs adaptive multimodal fusion based on class semantic similarity, yielding the final prediction result.

4 Experiments

We conduct an in-depth evaluation to the proposed method, including real-world practicality, generalization ability, multimodal fusion ability, ablation study, uncertainty analysis, and hyperparameter analysis.

4.1 Experimental Setup

Dataset. We conduct experiments on three multimodal audiovisual datasets: UCF, ActivityNet, and VGGSound [13]. For each dataset, we evenly divide the classes into two parts: the first part serves as seen classes for the audio modality (denoted A_s), while the second part serves as seen classes for the video modality (denoted B_s), maintaining the relationship where $\text{Classes}(A_s) = \text{Classes}(B_u)$ and $\text{Classes}(A_u) = \text{Classes}(B_s)$. During the training phase, the model exclusively utilizes data from A_s of the audio modality and B_s of the video modality for training.

Table 1: Comparison with SOTA methods in generalization ability, multimodal fusion ability and real-world scenarios. A_u and B_u represent the test results for unseen classes in single modality; $A_s + B_u$, $A_u + B_s$ and $A_{all} + B_{all}$ represent the test results for different category sets in complete modalities; acc_{mix} indicates the test results for mixed scenarios ($A_s, B_s, A_u, B_u, A_s + B_u, A_u + B_s$). For detailed descriptions of evaluation methods, please refer Appendix C.

Dataset	Methods		Generalization Ability		Multimodal Fusion Ability			Real-world Scenarios
			A_u	B_u	$A_s + B_u$	$A_u + B_s$	$A_{all} + B_{all}$	acc_{mix}
ActivityNet	ZSL	ZLA[IJCAI22] [66]	2.04	4.14	8.89	64.45	38.35	29.74
		DGZ[AAAI23] [1]	0.77	3.49	11.45	65.09	39.89	31.11
		DSECN[CVPR24] [8]	1.66	8.10	23.41	54.24	39.76	30.62
	MML	TMC[TPAMI22] [2]	0.00	0.00	17.25	69.11	44.75	32.72
		Mmdynamics[CVPR22] [36]	0.00	0.00	17.46	32.42	24.14	23.52
	IMV	LMVCAT[AAAI23] [5]	0.00	0.00	3.31	48.47	27.25	22.18
		UVaT[TIP24] [3]	0.00	0.00	41.30	33.82	37.34	35.48
CSCF (Ours)		3.96	11.20	48.61	84.33	67.55	45.71	
UCF	ZSL	ZLA[IJCAI22] [66]	9.73	6.89	56.39	74.62	65.48	51.51
		DGZ[AAAI23] [1]	4.81	8.68	70.36	54.76	48.02	50.74
		DSECN[CVPR24] [8]	4.31	6.69	68.46	40.12	54.33	44.91
	MML	TMC[TPAMI22] [2]	0.00	0.00	67.56	71.61	69.58	51.13
		Mmdynamics[CVPR22] [36]	0.00	0.00	61.88	45.34	52.78	47.89
	IMV	LMVCAT[AAAI23] [5]	0.00	0.00	57.29	63.19	60.23	48.67
		UVaT[TIP24] [3]	0.00	0.00	70.26	38.19	52.07	42.24
CSCF (Ours)		9.83	14.97	86.23	93.08	89.64	62.28	
VGGSound	ZSL	ZLA[IJCAI22] [66]	3.54	6.04	48.10	41.92	44.59	34.99
		DGZ[AAAI23] [1]	4.93	3.24	60.55	43.37	50.80	39.86
		DSECN[CVPR24] [8]	4.43	2.94	68.52	30.42	46.91	38.31
	MML	TMC[TPAMI22] [2]	0.00	0.00	64.44	49.80	56.14	41.80
		Mmdynamics[CVPR22] [36]	0.00	0.00	48.92	40.77	46.42	37.15
	IMV	LMVCAT[AAAI23] [5]	0.00	0.00	46.14	49.11	47.83	39.36
		UVaT[TIP24] [3]	0.00	0.00	68.37	19.89	40.87	38.30
CSCF (Ours)		8.74	8.65	69.31	60.97	64.58	45.10	

Table 2: Gradual improvement in the model’s fusion ability as the DMSS and CSMF modules are progressively added.

Dataset	Model	$A_s + B_u$	$A_u + B_s$	$A_{all} + B_{all}$
ActivityNet	B+O	45.70	82.39	65.15
	B+O+D	47.01(↑)	84.10(↑)	66.76(↑)
	B+O+D+C	48.61(↑)	84.33(↑)	67.55(↑)
UCF	B+O	83.83	90.07	86.94
	B+O+D	85.93(↑)	92.88(↑)	89.39(↑)
	B+O+D+C	86.23(↑)	93.08(↑)	89.64(↑)
VGGSound	B+O	66.24	58.77	60.36
	B+O+D	68.87(↑)	60.45(↑)	63.96(↑)
	B+O+D+C	69.31(↑)	60.97(↑)	64.58(↑)

Comparison. Seven state-of-the-art (SOTA) methods are selected for comparison with our proposed CSCF model. These methods include: Unimodal Zero-Shot Methods [66, 1, 8], Multimodal Classification Methods [2, 36] and Incomplete Multi-View Methods [5, 3]. For Unimodal Zero-Shot Methods, since multimodal capability is unsupported, we use a dual-model architecture: independent unimodal models are trained for modality A and modality B. During testing, the appropriate model is selected based on the input modality, and the result with higher confidence from the two models is chosen for multimodal inputs.

Implement Details. Implementation details are provided in Appendix D. The main codes and logs are provided in Supplementary Material.

4.2 Comparison with SOTA

We conduct a comprehensive comparison between our model and the state-of-the-art (SOTA) unimodal zero-shot methods, multimodal classification methods, and incomplete multi-view methods as follows.

Comprehensive Evaluation in Real-World Scenarios.

As shown in Table 1 (Real-world Scenarios). It can be observed that our method outperforms the best SOTA method by 10.23 points on ActivityNet dataset, demonstrating that our model exhibits stable predictive performance when dealing

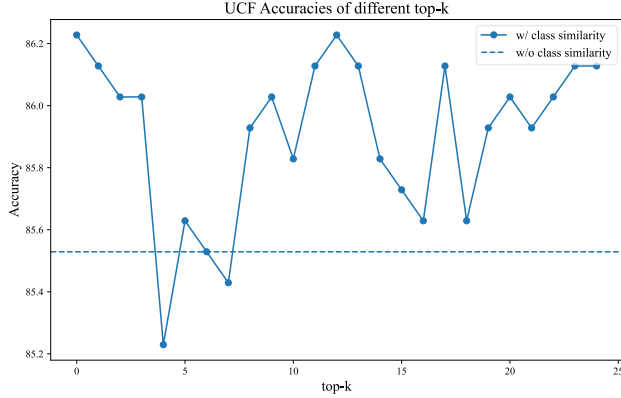


Figure 4: Analysis of the hyperparameter $top-k$ on the UCF dataset. "w/o class similarity" means no similarity fusion is used, while "w/ class similarity" indicates that similarity fusion is applied. We gradually increase the $top-k$ to observe its impact on the model's fusion capability.

with diverse modality combinations (unimodal/multimodal) and category distributions (seen classes/unseen classes) in the input data.

Generalization Ability Evaluation.

As shown in Table 1 (Generalization Ability). On the one hand, multimodal classification and incomplete view methods typically use fully connected layers as classification heads, which causes the model to be biased toward seen classes, resulting in a lack of generalization ability. On the other hand, our approach introduces large model-enhanced semantic representations as a bridge for cross-category knowledge transfer, establishing effective semantic associations between seen and unseen classes via distance metrics, significantly improving our model's zero-shot capability.

Multimodal Fusion Ability Evaluation.

As shown in Table 1 (Multimodal Fusion Ability). We conclude that: 1) Unseen class modality noise can disrupt model's decision-making, despite containing useful information; 2) The unimodal zero-shot methods that adopt an independent dual-model architecture process multimodal data by using a confidence selection strategy. However, unseen class modalities may produce overconfident predictions (see Appendix E for details), making it difficult to accurately identify the dominant modality; 3) Multimodal classification and incomplete view methods, due to the lack of cross-modal alignment supervision during training, struggle to establish effective inter-modal relationships; 4) Our method reliably identifies modality domains and dominant modalities, suppressing noise while leveraging similarity measures to extract useful unseen-class information for improved performance.

4.3 Ablation Study

Since our three modules each affect different functional aspects of the model, the experiment first quantitatively evaluates the contribution of each module to the overall performance in real-world scenarios, followed by a deeper analysis of the effectiveness of each module in specific functional dimensions. As shown in Figure 6, we observe that as the OSRS, DMSS, and CSMF modules are progressively integrated into the baseline model, the overall performance in real-world scenarios gradually improves, which strongly demonstrates the effectiveness of each module in enhancing the overall performance in real-world scenarios.

The effectiveness of the OSRS module on model generalization.

As shown in Figure 5, the OSRS module, compared to the traditional fully connected + Softmax classification method, significantly enhances the model's ability to recognize unseen categories through the semantic space alignment mechanism. Additionally, by incorporating semantic enhancement strategies, this module makes the category prototypes more representative within the shared semantic space, thereby further improving the model's generalization capability.

The effectiveness of the DMSS module on model fusion capability.

As shown in Table 2, compared to the simple modality prediction averaging fusion strategy, the DMSS module dynamically selects the dominant modality's prediction result through adaptive inconsistency estimation. This mechanism effectively suppresses the noise interference from unseen class data and enhances the model's robustness under MMHCL scenario.

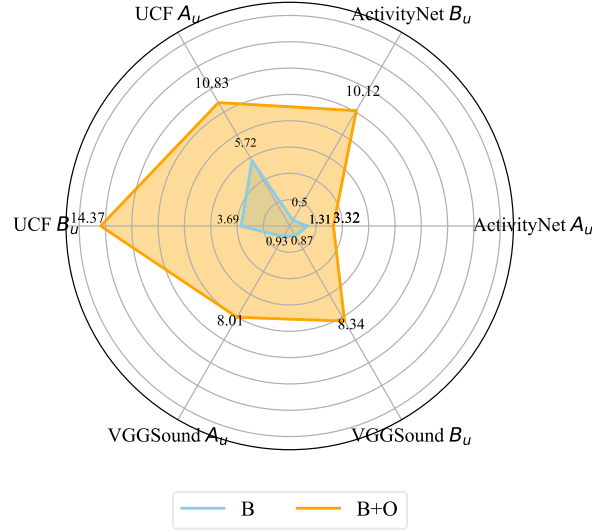


Figure 5: Comparison of the model’s ability to recognize unseen classes before and after introducing the OSRS module. "B+O" means adding the OSRS module to the baseline.

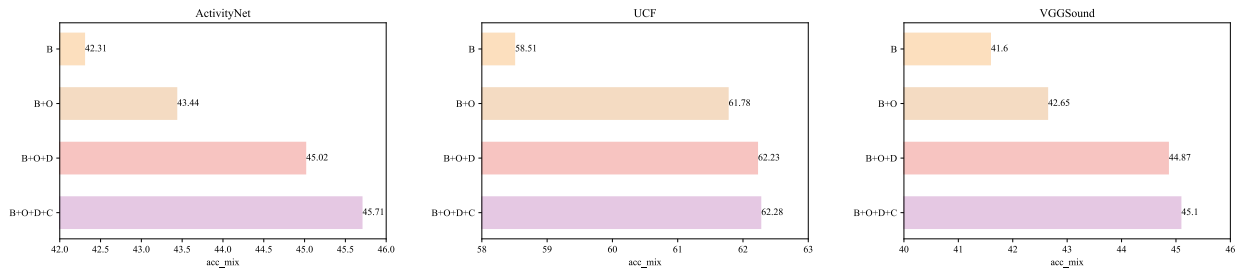


Figure 6: The impact of OSRS(O), DMSS(D), and CSMF(C) on the comprehensive performance of the model. We remove these three modules as our Baseline (B). In the ablation study, we add O, D, and C step by step to demonstrate their influence on the model’s overall performance.

The effectiveness of the CSMF module on model fusion capability. As shown in Table 2, directly selecting the dominant modality’s prediction result (without fusion) leads to the loss of some useful information. However, the CSMF module, through cross-modal similarity-weighted fusion, effectively utilizes the beneficial information from the auxiliary modality, thereby further enhancing the accuracy of multimodal decision-making.

4.4 Experimental Analysis

Comparison of Modality Prediction Uncertainty. By combining the intra-modal prediction inconsistency Inc^* mentioned in Section 3.2 with the inter-modal prediction discrepancy dif^* , we obtain the final modal prediction uncertainty u^* . We visualize the prediction uncertainty of each modality, as shown in Figure 7. It can be observed that, across 30 randomly selected samples, each modality exhibits low prediction uncertainty for its own seen classes, demonstrating high confidence in predictions. This suggests that these modalities can serve as the dominant ones in subsequent multimodal decision fusion.

Hyperparameter Analysis. As shown in Figure 4, as $top-k$ becomes smaller, the similarity weighting becomes more focused on the most relevant few categories. While increasing $top-k$ introduces more information from the unseen class modalities, it also brings in more noise.

5 Conclusion

In this paper, we propose an effective approach that aligns different modalities into a unified semantic space while integrating ensemble learning and class similarity, enabling a decision-making process driven by the dominant modality

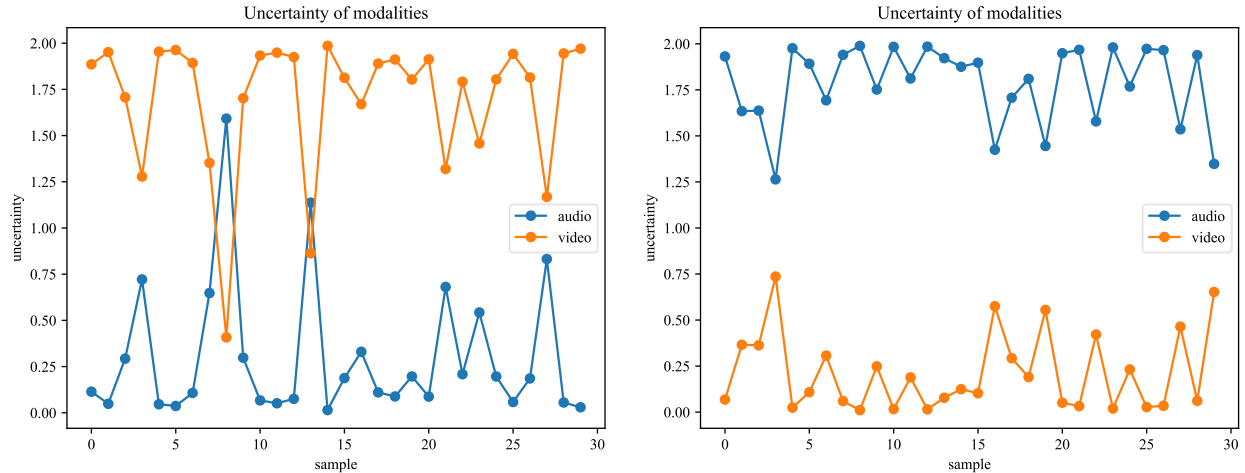


Figure 7: Comparison of prediction uncertainty across modalities. The horizontal axis represents 30 randomly selected samples, and the vertical axis represents the prediction uncertainty of each modality for the corresponding sample. The left subfigure presents the test results on the seen classes of the audio modality, while the right subfigure shows the test results on the seen classes of the video modality.

with auxiliary support from other modalities. From the experimental results, we draw the following key conclusions: 1) The MMHCL scenario is both practically significant and challenging. Existing generalized zero-shot learning methods, multimodal classification approaches, and incomplete-view methods experience significant performance degradation in this scenario; 2) Our model achieves strong generalization while effectively leveraging information from different modalities, performing well across various scenarios with a single training process. In the future, we will explore MMHCL methods based on federated learning, leveraging multi-center data while preserving privacy to further enhance model performance.

Potential Impact. The paper will help attract researchers’ attention to MMHCL and promote the development of multimodal learning toward a more practical direction. The proposed CSCF, by effectively integrating data from different projects and modalities, demonstrates outstanding generalization and multimodal fusion capabilities with just one training session. This property enables companies to maximize the use of data from various past projects, whether historical or cross-domain, providing rich training information for the model. As a result, the performance and robustness of the model are significantly enhanced, ultimately leading to the training of a more powerful model.

References

- [1] Dubing Chen, Yuming Shen, Haofeng Zhang, and Philip HS Torr. Deconstructed generation-based zero-shot model. In *AAAI*, volume 37, pages 295–303, 2023.
- [2] Zongbo Han, Changqing Zhang, Huazhu Fu, and Joey Tianyi Zhou. Trusted multi-view classification with dynamic evidential fusion. *IEEE TPAMI*, 45(2):2551–2566, 2023.
- [3] Yapeng Li, Yong Luo, and Bo Du. Uvat: Uncertainty incorporated view-aware transformer for robust multi-view classification. *IEEE Transactions on Image Processing*, 33:5129–5143, 2024.
- [4] Cai Xu, Yilin Zhang, Ziyu Guan, and Wei Zhao. Trusted multi-view learning with label noise, 2024.
- [5] Chengliang Liu, Jie Wen, Xiaoling Luo, and Yong Xu. Incomplete multi-view multi-label learning via label-guided masked view-and category-aware transformers. In *Proceedings of the AAAI conference on artificial intelligence*, volume 37, pages 8816–8824, 2023.
- [6] Wulin Xie, Xiaohuan Lu, Yadong Liu, Jiang Long, Bob Zhang, Shuping Zhao, and Jie Wen. Uncertainty-aware pseudo-labeling and dual graph driven network for incomplete multi-view multi-label classification. In *ACM MM*, MM '24, page 6656–6665, New York, NY, USA, 2024. Association for Computing Machinery.
- [7] Quanjiang Li, Tingjin Luo, Mingdie Jiang, Jiahui Liao, and Zhangqi Jiang. Deep incomplete multi-view network semi-supervised multi-label learning with unbiased loss. In *ACM MM*, MM '24, page 9048–9056, New York, NY, USA, 2024. Association for Computing Machinery.
- [8] Yapeng Li, Yong Luo, Zengmao Wang, and Bo Du. Improving generalized zero-shot learning by exploring the diverse semantics from external class names. In *CVPR*, pages 23344–23353, June 2024.
- [9] Shuhuang Chen, Dingjie Fu, Shiming Chen, Shuo Ye, Wenjin Hou, and Xinge You. Causal visual-semantic correlation for zero-shot learning. In *ACM MM*, MM '24, page 4246–4255, New York, NY, USA, 2024. Association for Computing Machinery.
- [10] Pratik Mazumder, Pravendra Singh, Kranti Kumar Parida, and Vinay P Namboodiri. Avgzslnet: Audio-visual generalized zero-shot learning by reconstructing label features from multi-modal embeddings. In *WACV*, pages 3090–3099, 2021.
- [11] Otniel-Bogdan Mercea, Lukas Riesch, A Koepke, and Zeynep Akata. Audio-visual generalised zero-shot learning with cross-modal attention and language. In *CVPR*, pages 10553–10563, 2022.
- [12] Jie Hong, Zeeshan Hayder, Junlin Han, Pengfei Fang, Mehrtash Harandi, and Lars Petersson. Hyperbolic audio-visual zero-shot learning. In *ICCV*, pages 7873–7883, 2023.
- [13] David Kurzendörfer, Otniel-Bogdan Mercea, A. Sophia Koepke, and Zeynep Akata. Audio-visual generalized zero-shot learning using pre-trained large multi-modal models. In *CVPR*, pages 2627–2638, June 2024.
- [14] Dhanesh Ramachandram and Graham W Taylor. Deep multimodal learning: A survey on recent advances and trends. *IEEE signal processing magazine*, 34(6):96–108, 2017.
- [15] Tadas Baltrušaitis, Chaitanya Ahuja, and Louis-Philippe Morency. Multimodal machine learning: A survey and taxonomy. *IEEE TPAMI*, 41(2):423–443, 2019.
- [16] Yang Wang. Survey on deep multi-modal data analytics: Collaboration, rivalry, and fusion. *ACM Transactions on Multimedia Computing, Communications, and Applications (TOMM)*, 17(1s):1–25, 2021.
- [17] William C Sleeman IV, Rishabh Kapoor, and Preetam Ghosh. Multimodal classification: Current landscape, taxonomy and future directions. *ACM Computing Surveys*, 55(7):1–31, 2022.
- [18] Meng Shen, Yizheng Huang, Jianxiong Yin, Heqing Zou, Deepu Rajan, and Simon See. Towards balanced active learning for multimodal classification. In *ACM MM*, MM '23, page 3434–3445, New York, NY, USA, 2023. Association for Computing Machinery.
- [19] Maarten Sukel, Stevan Rudinac, and Marcel Worring. Multimodal classification of urban micro-events. In *ACM MM*, MM '19, page 1455–1463, New York, NY, USA, 2019. Association for Computing Machinery.
- [20] Yuwei Zhou, Xin Wang, Hong Chen, Xuguang Duan, and Wenwu Zhu. Intra- and inter-modal curriculum for multimodal learning. In *ACM MM*, MM '23, page 3724–3735, New York, NY, USA, 2023. Association for Computing Machinery.
- [21] Stevan Rudinac, Iva Gornishka, and Marcel Worring. Multimodal classification of violent online political extremism content with graph convolutional networks. In *ACM MM*, Thematic Workshops '17, page 245–252, New York, NY, USA, 2017. Association for Computing Machinery.

- [22] Soujanya Poria, Erik Cambria, and Alexander Gelbukh. Deep convolutional neural network textual features and multiple kernel learning for utterance-level multimodal sentiment analysis. In *Proceedings of the 2015 conference on empirical methods in natural language processing*, pages 2539–2544, 2015.
- [23] Cinmayii A Garillos-Manliguez and John Y Chiang. Multimodal deep learning and visible-light and hyperspectral imaging for fruit maturity estimation. *Sensors*, 21(4):1288, 2021.
- [24] John Arevalo, Thamar Solorio, Manuel Montes-y Gómez, and Fabio A González. Gated multimodal units for information fusion. *arXiv preprint arXiv:1702.01992*, 2017.
- [25] Douwe Kiela, Suvrat Bhooshan, Hamed Firooz, Ethan Perez, and Davide Testuggine. Supervised multimodal bitransformers for classifying images and text. *arXiv preprint arXiv:1909.02950*, 2019.
- [26] Yao-Hung Hubert Tsai, Shaojie Bai, Paul Pu Liang, J Zico Kolter, Louis-Philippe Morency, and Ruslan Salakhutdinov. Multimodal transformer for unaligned multimodal language sequences. In *Proceedings of the conference. Association for computational linguistics. Meeting*, volume 2019, page 6558. NIH Public Access, 2019.
- [27] Danfeng Hong, Lianru Gao, Naoto Yokoya, Jing Yao, Jocelyn Chanussot, Qian Du, and Bing Zhang. More diverse means better: Multimodal deep learning meets remote-sensing imagery classification. *IEEE Transactions on Geoscience and Remote Sensing*, 59(5):4340–4354, 2021.
- [28] Jian Huang, Jianhua Tao, Bin Liu, Zheng Lian, and Mingyue Niu. Multimodal transformer fusion for continuous emotion recognition. In *ICASSP*, pages 3507–3511. IEEE, 2020.
- [29] Yikai Wang, Wenbing Huang, Fuchun Sun, Tingyang Xu, Yu Rong, and Junzhou Huang. Deep multimodal fusion by channel exchanging. In H. Larochelle, M. Ranzato, R. Hadsell, M.F. Balcan, and H. Lin, editors, *NeurIPS*, volume 33, pages 4835–4845. Curran Associates, Inc., 2020.
- [30] Ronghang Hu and Amanpreet Singh. Unit: Multimodal multitask learning with a unified transformer. In *ICCV*, pages 1439–1449, 2021.
- [31] Yu Huang, Chenzhuang Du, Zihui Xue, Xuanyao Chen, Hang Zhao, and Longbo Huang. What makes multi-modal learning better than single (provably). In *NeurIPS*, volume 34, pages 10944–10956, 2021.
- [32] Changhee Lee and Mihaela Van der Schaar. A variational information bottleneck approach to multi-omics data integration. In *International Conference on Artificial Intelligence and Statistics*, pages 1513–1521. PMLR, 2021.
- [33] Hang Li, Fan Yang, Xiaohan Xing, Yu Zhao, Jun Zhang, Yueping Liu, Mengxue Han, Junzhou Huang, Liansheng Wang, and Jianhua Yao. Multi-modal multi-instance learning using weakly correlated histopathological images and tabular clinical information. In *MICCAI*, pages 529–539. Springer, 2021.
- [34] Pradeep Natarajan, Shuang Wu, Shiv Vitaladevuni, Xiaodan Zhuang, Stavros Tsakalidis, Unsang Park, Rohit Prasad, and Premkumar Natarajan. Multimodal feature fusion for robust event detection in web videos. In *CVPR*, pages 1298–1305, 2012.
- [35] Mahesh Subedar, Ranganath Krishnan, Paulo Lopez Meyer, Omesh Tickoo, and Jonathan Huang. Uncertainty-aware audiovisual activity recognition using deep bayesian variational inference. In *ICCV*, pages 6301–6310, 2019.
- [36] Zongbo Han, Fan Yang, Junzhou Huang, Changqing Zhang, and Jianhua Yao. Multimodal dynamics: Dynamical fusion for trustworthy multimodal classification. In *CVPR*, pages 20707–20717, June 2022.
- [37] Haojian Huang, Chuanyu Qin, Zhe Liu, Kaijing Ma, Jin Chen, Han Fang, Chao Ban, Hao Sun, and Zhongjiang He. Trusted unified feature-neighborhood dynamics for multi-view classification. *arXiv preprint arXiv:2409.00755*, 2024.
- [38] Yarin Gal and Zoubin Ghahramani. Dropout as a bayesian approximation: Representing model uncertainty in deep learning. In Maria Florina Balcan and Kilian Q. Weinberger, editors, *Proceedings of The 33rd International Conference on Machine Learning*, volume 48 of *Proceedings of Machine Learning Research*, pages 1050–1059, New York, New York, USA, 20–22 Jun 2016. PMLR.
- [39] Murat Sensoy, Lance Kaplan, and Melih Kandemir. Evidential deep learning to quantify classification uncertainty. In *NeurIPS*, volume 31, 2018.
- [40] Alexander Lyzhov, Yuliya Molchanova, Arsenii Ashukha, Dmitry Molchanov, and Dmitry Vetrov. Greedy policy search: A simple baseline for learnable test-time augmentation. In Jonas Peters and David Sontag, editors, *Proceedings of the 36th Conference on Uncertainty in Artificial Intelligence (UAI)*, volume 124 of *Proceedings of Machine Learning Research*, pages 1308–1317. PMLR, 03–06 Aug 2020.
- [41] Emilie Morvant, Amaury Habrard, and Stéphane Ayache. Majority vote of diverse classifiers for late fusion. In Pasi Fränti, Gavin Brown, Marco Loog, Francisco Escolano, and Marcello Pelillo, editors, *Structural, Syntactic, and Statistical Pattern Recognition*, pages 153–162, Berlin, Heidelberg, 2014. Springer Berlin Heidelberg.

- [42] Ekaterina Shutova, Douwe Kiela, and Jean Maillard. Black holes and white rabbits: Metaphor identification with visual features. In *Proceedings of the 2016 conference of the North American chapter of the association for computational linguistics: Human language technologies*, pages 160–170, 2016.
- [43] G. Potamianos, C. Neti, G. Gravier, A. Garg, and A.W. Senior. Recent advances in the automatic recognition of audiovisual speech. *Proceedings of the IEEE*, 91(9):1306–1326, 2003.
- [44] Michael Glodek, Stephan Tschechne, Georg Layher, Martin Schels, Tobias Brosch, Stefan Scherer, Markus Kächele, Miriam Schmidt, Heiko Neumann, Günther Palm, et al. Multiple classifier systems for the classification of audio-visual emotional states. In *Affective Computing and Intelligent Interaction: Fourth International Conference, ACII 2011, Memphis, TN, USA, October 9–12, 2011, Proceedings, Part II*, pages 359–368. Springer, 2011.
- [45] Geovany A. Ramirez, Tadas Baltrušaitis, and Louis-Philippe Morency. Modeling latent discriminative dynamic of multi-dimensional affective signals. In Sidney D’Mello, Arthur Graesser, Björn Schuller, and Jean-Claude Martin, editors, *Affective Computing and Intelligent Interaction*, pages 396–406, Berlin, Heidelberg, 2011. Springer Berlin Heidelberg.
- [46] Natasha Jaques, Sara Taylor, Akane Sano, and Rosalind Picard. Multi-task, multi-kernel learning for estimating individual wellbeing. In *Proc. NIPS Workshop on Multimodal Machine Learning, Montreal, Quebec*, volume 898, page 3, 2015.
- [47] Luan Tran, Xiaoming Liu, Jiayu Zhou, and Rong Jin. Missing modalities imputation via cascaded residual autoencoder. In *CVPR*, July 2017.
- [48] Chao Shang, Aaron Palmer, Jiangwen Sun, Ko-Shin Chen, Jin Lu, and Jinbo Bi. Vigan: Missing view imputation with generative adversarial networks. In *2017 IEEE International Conference on Big Data (Big Data)*, pages 766–775, 2017.
- [49] Jiacheng Jiang, Hong Tao, Ruidong Fan, Wenzhang Zhuge, and Chenping Hou. Incomplete multi-view learning via half-quadratic minimization. *Neurocomputing*, 443:106–116, 2021.
- [50] Changqing Zhang, Zongbo Han, yajie cui, Huazhu Fu, Joey Tianyi Zhou, and Qinghua Hu. Cpm-nets: Cross partial multi-view networks. In H. Wallach, H. Larochelle, A. Beygelzimer, F. d’Alché-Buc, E. Fox, and R. Garnett, editors, *Advances in Neural Information Processing Systems*, volume 32. Curran Associates, Inc., 2019.
- [51] Xiang Li and Songcan Chen. A concise yet effective model for non-aligned incomplete multi-view and missing multi-label learning. *IEEE Transactions on Pattern Analysis and Machine Intelligence*, 44(10):5918–5932, 2022.
- [52] Zhenyong Fu, Tao Xiang, Elyor Kodirov, and Shaogang Gong. Zero-shot learning on semantic class prototype graph. *IEEE Transactions on Pattern Analysis and Machine Intelligence*, 40(8):2009–2022, 2018.
- [53] Li Niu, Jianfei Cai, Ashok Veeraraghavan, and Liqing Zhang. Zero-shot learning via category-specific visual-semantic mapping and label refinement. *IEEE Transactions on Image Processing*, 28(2):965–979, 2019.
- [54] Yanan Li, Donghui Wang, Huanhang Hu, Yuetan Lin, and Yueting Zhuang. Zero-shot recognition using dual visual-semantic mapping paths. In *CVPR*, July 2017.
- [55] Fei Zhang and Guangming Shi. Co-representation network for generalized zero-shot learning. In Kamalika Chaudhuri and Ruslan Salakhutdinov, editors, *ICML*, volume 97 of *Proceedings of Machine Learning Research*, pages 7434–7443. PMLR, 09–15 Jun 2019.
- [56] Ivan Skorokhodov and Mohamed Elhoseiny. Class normalization for (continual)? generalized zero-shot learning, 2021.
- [57] Shiming Chen, Ziming Hong, Guo-Sen Xie, Wenhan Yang, Qinmu Peng, Kai Wang, Jian Zhao, and Xinge You. Msdn: Mutually semantic distillation network for zero-shot learning. In *CVPR*, pages 7612–7621, June 2022.
- [58] Zhi Chen, Pengfei Zhang, Jingjing Li, Sen Wang, and Zi Huang. Zero-shot learning by harnessing adversarial samples. In *ACM MM*, pages 4138–4146, 2023.
- [59] Rui Gao, Xingsong Hou, Jie Qin, Jiaxin Chen, Li Liu, Fan Zhu, Zhao Zhang, and Ling Shao. Zero-vae-gan: Generating unseen features for generalized and transductive zero-shot learning. *IEEE Transactions on Image Processing*, 29:3665–3680, 2020.
- [60] Akanksha Paul, Narayanan C. Krishnan, and Prateek Munjal. Semantically aligned bias reducing zero shot learning. In *CVPR*, June 2019.
- [61] Jiamin Wu, Tianzhu Zhang, Zheng-Jun Zha, Jiebo Luo, Yongdong Zhang, and Feng Wu. Self-supervised domain-aware generative network for generalized zero-shot learning. In *CVPR*, June 2020.
- [62] Yongqin Xian, Tobias Lorenz, Bernt Schiele, and Zeynep Akata. Feature generating networks for zero-shot learning. In *CVPR*, June 2018.

- [63] Edgar Schonfeld, Sayna Ebrahimi, Samarth Sinha, Trevor Darrell, and Zeynep Akata. Generalized zero- and few-shot learning via aligned variational autoencoders. In *CVPR*, June 2019.
- [64] Sanath Narayan, Akshita Gupta, Fahad Shahbaz Khan, Cees GM Snoek, and Ling Shao. Latent embedding feedback and discriminative features for zero-shot classification. In *ECCV*, pages 479–495. Springer, 2020.
- [65] Shiming Chen, Wenjie Wang, Beihao Xia, Qinmu Peng, Xinge You, Feng Zheng, and Ling Shao. Free: Feature refinement for generalized zero-shot learning. In *ICCV*, pages 122–131, October 2021.
- [66] Dubing Chen, Yuming Shen, Haofeng Zhang, and Philip H.S. Torr. Zero-shot logit adjustment. In Lud De Raedt, editor, *IJCAI*, pages 813–819, 7 2022. Main Track.
- [67] Shiming Chen, Wenjin Hou, Ziming Hong, Xiaohan Ding, Yibing Song, Xinge You, Tongliang Liu, and Kun Zhang. Evolving semantic prototype improves generative zero-shot learning. In Andreas Krause, Emma Brunskill, Kyunghyun Cho, Barbara Engelhardt, Sivan Sabato, and Jonathan Scarlett, editors, *Proceedings of the 40th International Conference on Machine Learning*, volume 202 of *Proceedings of Machine Learning Research*, pages 4611–4622. PMLR, 23–29 Jul 2023.
- [68] Josh Achiam, Steven Adler, Sandhini Agarwal, Lama Ahmad, Ilge Akkaya, Florencia Leoni Aleman, Diogo Almeida, Janko Altenschmidt, Sam Altman, Shyamal Anadkat, et al. Gpt-4 technical report. *arXiv preprint arXiv:2303.08774*, 2023.
- [69] Chuanxing Geng, Sheng-Jun Huang, and Songcan Chen. Recent advances in open set recognition: A survey. *IEEE TPAMI*, 43(10):3614–3631, 2021.
- [70] Omer Sagi and Lior Rokach. Ensemble learning: A survey. *Wiley interdisciplinary reviews: data mining and knowledge discovery*, 8(4):e1249, 2018.

Table 3: Examples of class description generated by SA. The blue and purple sentences are audio and video feature.

Original Class Name	Class Description
Swimming	The rhythmic splash of strokes and the occasional gasp for air. A swimmer cutting through the water.
Cat purring	The soothing, vibrating hum of a content cat. A relaxed feline curling up in a cozy spot.
Cleaningshoes	The squeak of a brush against leather. Shoes being polished to a glossy shine.
Knitting	The click-clack of knitting needles and the soft pull of yarn. A colorful scarf or sweater taking shape on someone’s lap.

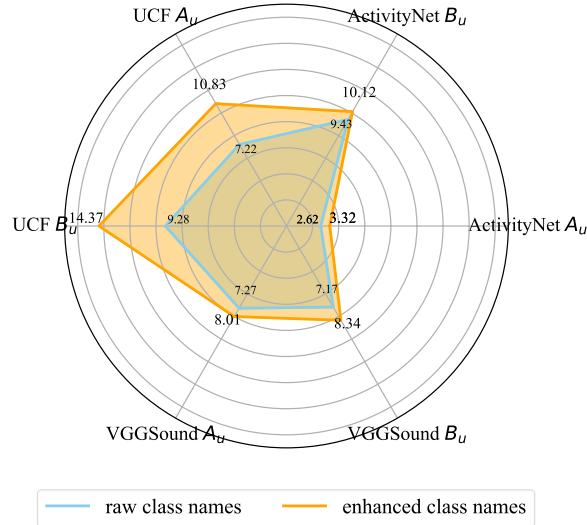


Figure 8: Comparison of the model(B+O)’s ability to recognize unseen classes before and after incorporating semantic enhancement.

A Semantic Enhancement

We have designed a prompt-based strategy to guide the large language model (LLM) in transforming category names into descriptive statements that capture their attributes, thereby generating richer and more informative semantic features. The generated statements are then used as input to extract semantic features. Formally, the extraction of enhanced semantic features for category names is as follows:

$$c_i = CLIP(LLM(Y_i)) \tag{11}$$

Using a large language model (LLM), we transform the original category names into descriptive sentences, as shown in Table 3. It can be observed that, compared to the raw category names, the sentence descriptions contain richer visual and auditory information, which helps enhance the transfer from seen to unseen categories.

We conduct an ablation study on the semantic enhancement module based on the B+O model, as shown in Figure 8. It can be observed that incorporating semantic enhancement significantly improves the model’s ability to recognize unseen classes compared to the version without semantic enhancement.

B The Inconsistency in Intra-Modal Predictions

We adopt an ensemble learning strategy by training four OSRS modules with different architectures within each modality and randomly select 30 samples for testing. As shown in Figure 9, each polyline represents the predictions from a sub-network for the 30 samples. The right plot displays predictions for seen classes in the video modality, where the high overlap of polylines indicates strong prediction consistency among the four OSRS modules. In contrast, the left plot shows predictions for unseen classes in the audio modality, with less polyline overlap, revealing lower consistency across the modules.

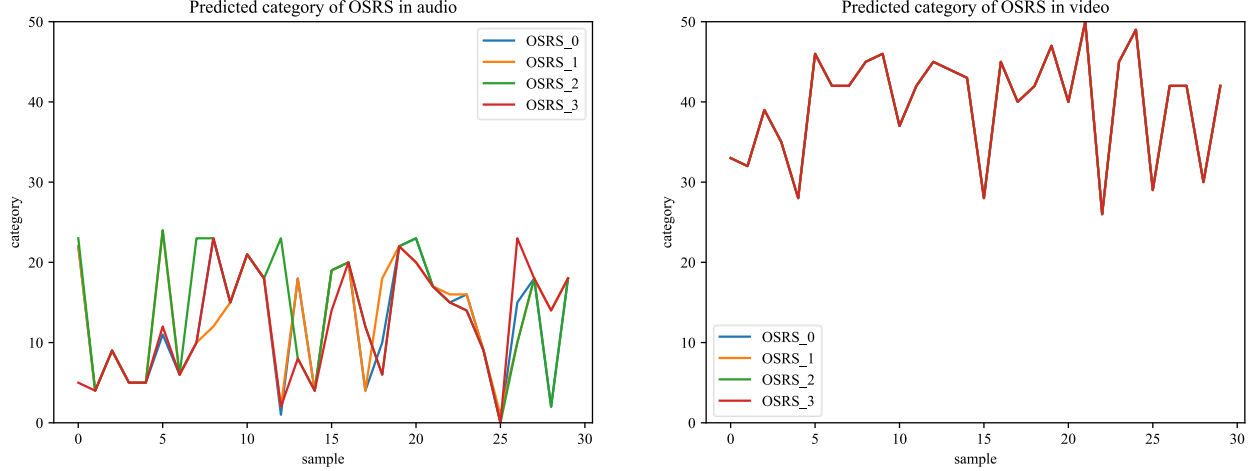


Figure 9: The predictions of each OSRS module within individual modalities are illustrated. The x-axis represents the 30 randomly selected samples, while the y-axis indicates the predicted categories.

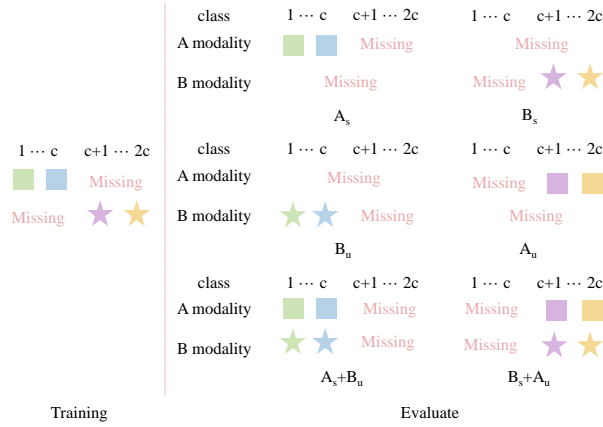


Figure 10: Visualization of the existence states of multimodal data during training and evaluate.

C Evaluation Methods

We evaluate three key aspects: real-world applicability, generalization ability (for Challenge 1), and multimodal fusion ability (for Challenges 2-3).

Real-world Scenarios Evaluation

- Unimodal seen class testing (A_s, B_s)
- Unimodal unseen class testing (A_u, B_u)
- Cross-modal mixed testing ($A_s + B_u, B_s + A_u$)

Generalization Ability Evaluation

- Modality A unseen class testing (A_u)
- Modality B unseen class testing (B_u)

Multimodal Fusion Ability Evaluation

- Modality A seen class + Modality B unseen class ($A_s + B_u$)
- Modality B seen class + Modality A unseen class ($B_s + A_u$)

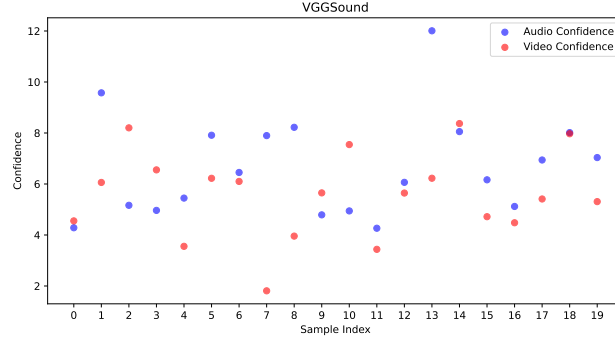


Figure 11: Confidence levels of two zero-shot models trained separately on audio and video modalities during full-modality testing. Despite the audio modality not having encountered these classes, certain samples still exhibit high audio confidence. Blue dots indicate audio confidence, while red dots indicate video confidence.

The diagrams of A_s , B_s , A_u , B_u , $A_s + B_u$, $B_s + A_u$ are shown in Figure 10.

D Implementation Details

For the audio and visual features of ActivityNet, UCF, and VGGSound ($d^a = 1024$ and $d^v = 512$), we use features extracted by CLIPCLAP [13]. Missing modality data is padded with zero vectors (1024-D for audio and 512-D for video). The semantic embeddings of the classes are obtained using the CLIP ViT-B/32 text encoder ($d^s = 512$). We train our model using the Adam optimizer with a learning rate of 5×10^{-4} and weight decay of 10^{-4} . The training epoch and batch size are set to 50 and 256, respectively. Our model is implemented in PyTorch. All experiments are conducted under the same hardware environment, including an NVIDIA GeForce RTX 4090 GPU, an Intel Core i9-13900K CPU, and 128 GB of RAM.

E Confidence Analysis

As shown in Figure 11, for two zero-shot models trained separately on audio and video modalities, we randomly sampled twenty instances from classes that were only seen in the video modality during training. The results reveal that although these classes were unseen in the audio modality, the model still produces overconfident predictions for certain samples.